Theory of Oxygen-Boron Vacancy Defect in Cubic Boron Nitride: A Diamond NV^{-} Isoelectronic Center

Tesfaye A. Abtew, Weiwei Gao, Xiang Gao, Y. Y. Sun, S. B. Zhang, and Peihong Zhang

Phys. Rev. Lett. **113**, 136401 — Published 23 September 2014

DOI: 10.1103/PhysRevLett.113.136401

Theory of oxygen-boron vacancy defect in cubic boron nitride: A diamond NV^- isoelectronic center

Tesfaye A. Abtew[1], Weiwei Gao[1], Xiang Gao[2], Y. Y. Sun[3], S. B. Zhang[3], and Peihong Zhang[1,2]
[1]*Department of Physics, University at Buffalo, State University of New York, Buffalo, New York 14260, USA*
[2]*Beijing Computational Science Research Center, Beijing 100084, China and*
[3]*Department of Physics, Applied Physics and Astronomy, Rensselaer Polytechnic Institute, Troy, New York 12180, USA*
(Dated: August 28, 2014)

A color center in *c*-BN which is isoelectronic to diamond NV^- is predicted based on first-principles electronic structure calculations using the Heyd-Scuseria-Ernzerhof hybrid functional. The defect consists of an substitutional oxygen and an adjacent boron vacancy (O_N-V_B). We find that the O_N-V_B center is optically accessible with a zero-phonon-line of about 1.6 eV. The O_N-V_B center also shares much of the characteristics of the GC-2 center often observed in *c*-BN. A prominent vibronic coupling peak is predicted to be around 55 meV, which is in excellent agreement with the characteristic phonon frequency (56 meV) observed in the luminescence spectra of the GC-2 center.

A successful transition from a transistor-based computing paradigm to quantum computing requires identifying systems with desired properties such as having a long quantum coherence time and being scalable. In this regard, the negatively charged nitrogen-vacancy (NV^-) center in diamond, with its unique spin and optical properties, has emerged as a promising solid system for quantum information applications. The promises of the NV^- center have inspired unprecedented research interests in optical manipulations of defect states, and have fostered the search for alternative isoelectronic defect systems.[1] Since cubic boron nitride (*c*-BN) shares many of the interesting properties with diamond, it is likely the best system to host an NV^-−like isoelectronic defect center. In the past, technical difficulties in growing high quality and thick *c*-BN films had limited its potentials. Recently, however, there are very encouraging developments in the synthesis and annealing techniques, [2–8] thereby prompting renewed interest in this material.

In this letter, we predict a diamond NV^- like color center in *c*-BN. This defect center consists of a substitutional oxygen and an adjacent boron vacancy, O_N-V_B (shown in Fig. 1), and displays most of the interesting properties found in the NV^- center . We find that the electronic structure of the O_N-V_B center resembles that of the NV^- center in diamond, thus providing a potential alternative to the NV^- center. The O_N-V_B center is optically accessible with a zero-phonon-line of about 1.6 eV, to be compared with 1.95 eV for the NV^- center. The O_N-V_B center also shares much of the characteristics of the GC-2 center often observed in *c*-BN.[9–13]

Experimentally, optical properties of defects in *c*-BN have been investigated using photoluminescence (PL) and cathodoluminescence (CL) techniques.[9–15] Identification of defect center in *c*-BN using electron spin resonance (ESR) experiments have also been reported. [16, 17] Surprisingly, to the best of our knowledge, there has been no reported work using optically detected magnetic resonance to characterize defect centers in c-BN. From the CL measurements, vibronic spectra of three defect centers, labelled GC-1, GC-2, and GC-3 with ZPL of 1.76 eV, 1.63 eV, and 1.55 eV, respectively, have been identified.[9] It is suggested that GC-1 be vacancy-related, while GC-2 be a vacancy complex.[9–11] The precise origin of these centers, however, have not been clearly identified. The measured energy of the ZPL of the GC-2 center agrees well with our theoretical value of 1.60 eV. Our assignment that the O_N-V_B be the observed GC-2 center is also consistent with the understanding that the GC-2 is a vacancy complex. In addition, the measured characteristic phonon frequency accompanied by the cathodoluminescence of the GC-2 center is about 56 meV [10, 12] which is in excellent agreement with our theoretical estimate of 55 meV.

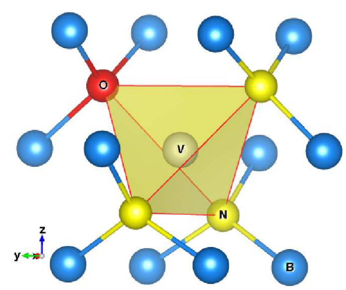

FIG. 1: (Color online) Structure of a O_N-V_B center in *c*-BN. Nitrogen atoms are shown in yellow (light color), boron in blue, and oxygen in red (dark). The boron vacancy (V_B) at the center of the tetrahedron is also shown.

Our density functional theory (DFT) calculations are carried out using the QUANTUM ESPRESSO package.[18] Optical excitation energies of the O_N-V_B center are calculated within the well-established constrained DFT approach using the Heyd-Scuseria-Ernzerhof (HSE06) hybrid functional.[19] For comparison, we have also used the Perdew-Burke-Ernzerhof (PBE) functional [20]) in our calculations. A 50 Ry energy cutoff is used for the planewave expansion of the wave functions, and 500 Ry is used for the charge density. We use a supercell containing 216 atoms to characterize the electronic and phonon properties of the defect using a Γ-point sampling scheme. We believe that our model is sufficiently large that important features of this defect can be captured. For example, we observe nearly dispersionless in-gap defect states for both diamond NV^- and the $O_N{-}V_B$ centers, indicating negligible interactions between periodic defect images. The structures are fully relaxed both for the ground state occupation and the constrained excited state occupation.

The $O_N{-}V_B$ defect complex introduces substantial local structural changes: The volume of the tetrahedron formed by the substitutional oxygen atom and the three nitrogen atoms surrounding the vacancy expands by about 27% calculated within the HSE06 functional. The O-B and the N-B bond lengths near the vacancy shorten by about 2% and 3%, respectively, relative to the ideal B-N bond length. This local structural relaxation is very similar to that in the NV^- center in diamond for which the N-C and the C-C bonds near the vacancy shrink by about 4% and 3% compared to the ideal C-C bond length in diamond. We have also investigated

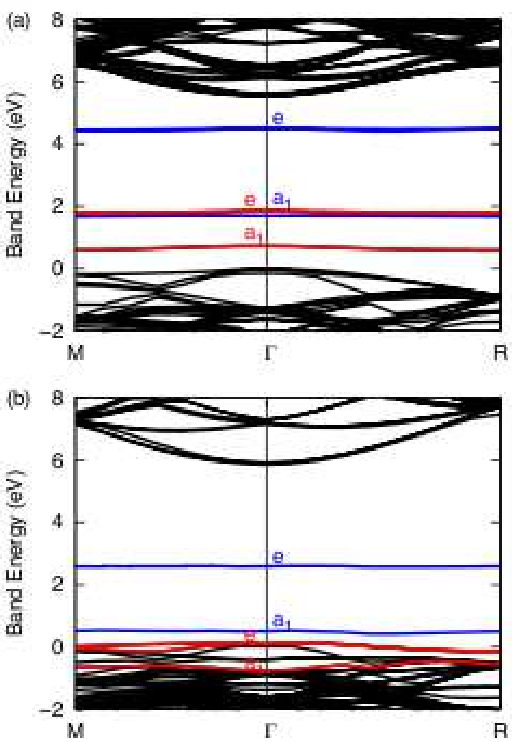

FIG. 2: (Color online) Band structures of (a) NV^- center in diamond, and (b) $O_N{-}V_B$ center in c-BN calculated using a 216-atom supercell and the HSE06 functional. The spin resolved defect states (e and a_1) are shown in red and blue lines for the majority and minority spins, respectively.

the stability of the neutral $O_N{-}V_B$ defect complex and find that that the neutral defect is stable as long as the Fermi level lies within 2 eV (see Supplemental Material) from the valence band maximum (VBM). Since c-BN can be both $p-$ and $n-$doped [21], it is possible to tune the Fermi level across the band gap so that the above condition can be achieved.

Figure 2 compares the electronic structures of an NV^- and an $O_N{-}V_B$ center calculated using the HSE06 functional with a 216-atom supercell. The calculated band gap is about 6.0 eV for c-BN within the HSE06 functional, this compares well with the recently measured value of 6.4 eV [22] for the minimum gap of c-BN. Similar to the NV^- center in diamond, the $O_N{-}V_B$ center also introduces optically active defect states, i.e., occupied a_1 and unoccupied e minority-spin states (shown in blue in the figure), deep inside the band gap, thereby enabling optical probe and/or control of the defect states. The ground state of the $O_N{-}V_B$ center is a spin triplet with an electronic configuration $(a_1^2e^2)[^3A_2]$, which is identical to that of the NV^- center. The optically inactive majority-spin defect states, however, show significant difference between the two systems: whereas the majority-spin defect states for the NV^- center are well isolated and located inside the band gap, those for the $O_N{-}V_B$ center seem to be in resonance with bulk valence states. As far as optical probe of defect states is concerned, however, the $O_N{-}V_B$ and NV^- defect centers should show very similar behavior since only minority-spin states are involved in spin-conserving optical excitations.

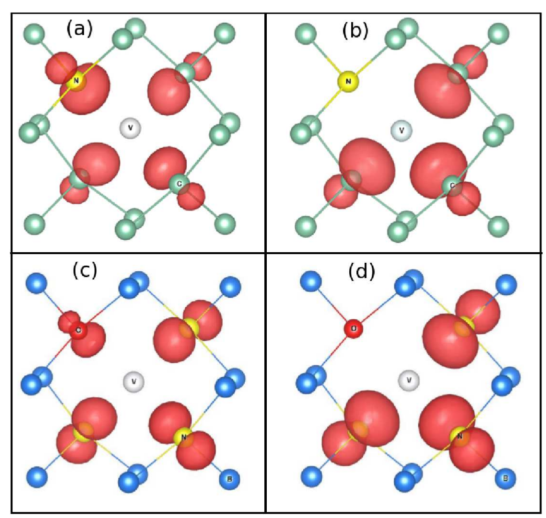

FIG. 3: (Color online) Charge density plots for the minority-spin a_1 [(a) and (c)] and e [(b) and (d)] defect states for the NV^- center in diamond and the $O_N{-}V_B$ center in c-BN, respectively. Only atoms near the defect center are shown for clarity. The value of the charge density for the isosurface plot is 1.0×10^{-2} e/a_0^3.

The localization of defect states is illustrated in Fig. 3, which compares the minority-spin a_1 and e defect states in the NV$^-$ and the O_N-V_B centers calculated within the HSE06 functional. For the NV$^-$ center, the a_1 state [Fig. 3(a)] is primarily localized on the substitutional nitrogen and on the three carbon atoms near the vacancy; the e doublet [Fig. 3(b)], on the other hand, is highly localized on the three carbon atoms around the vacancy, and has no contribution from the substitutional nitrogen. The defect states of the O_N-V_B center display similar behaviors to those of the NV$^-$ center: the a_1 state [3(c)] is localized on the substitutional oxygen and the three nearby nitrogen atoms, and the e state [Fig. 3(d)] is highly localized only on the three nitrogen atoms near the vacancy.

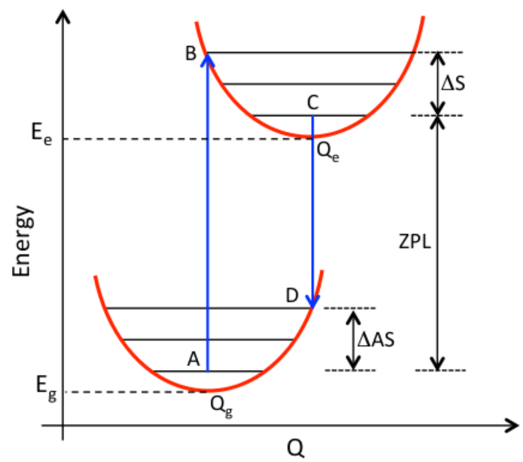

FIG. 4: Schematic for the energy versus configuration coordinate Q for two electronic states involved in optical transitions within the Franck-Condon principle.

The optical properties of the NV$^-$ center have been investigated in great details. For example, the ZPL is measured to be 1.945 eV,[23] and the Stokes shift (ΔS) and the anti-Stokes shift (ΔAS) are 235 meV and 185 meV, respectively. A schematic illustration of the optical transitions of a defect center is shown in Fig. 4. For the GC-2 center, however, only the ZPL (1.63 eV) and the characteristic phonon frequency (56 meV) have been identified.[10, 12] Theoretically, the optical transitions of defect states can be approximated by the total energy difference between the two electronic states involved within the Franck-Condon principle using the constrained DFT approach. For example, the energy of the vertical transition A→B (Fig. 4) can be calculated using the total energy of the excited state and that of the ground state within DFT, i.e, $\Delta E(\mathrm{A}\to\mathrm{B}) = E_e(\mathrm{Q_g}) - E_g(\mathrm{Q_g})$, where the energy of the excited state is calculated using the ground state structural configuration Q_g but with a constrained occupation by promoting one electron from the minority-spin a_1 to the minority-spin e state. Similarly, the energy of the vertical transition C→D is calculated using the excited state structural configuration Q_e, i.e., structure relaxed with the excited state occupation. Within this approximation, the transition A→C (or C→A) gives rise to ZPL assuming that the zero-point phonon energies are the same for both the ground state and the excited state. The Stokes shift ΔS and the anti-Stokes shift ΔAS can also be estimated as illustrated in Fig. 4.

Table I compares the optical transitions of the NV$^-$ center in diamond and those of the O_N-V_B in c-BN. The accuracy of the HSE06 functional in the prediction of the optical transitions of highly localized defects such as the NV$^-$ center has been previously demonstrated,[24] as we have quoted in the table. For example, the calculated energy of the ZPL for the NV$^-$ center is about 1.96 eV, to be compared with the experimental value of 1.95 eV.[24] Our calculated ZPL for O_N-V_B is 1.60 eV, which is very close to the measured value (1.63 eV) of the GC-2 center in c-BN. For comparison, we also included results calculated using the PBE functional. As we have mentioned earlier, the precise nature of the GC-2 defect center in c-BN is still not well characterized experimentally. To the best of our knowledge, there have been no measurements of the Stokes shift ΔS and the anti-Stokes shift ΔAS for the GC-2 center. Therefore, our results call for future experimental verification.

TABLE I: Optical transition energies for the O_N-V_B center in c-BN and the NV$^-$ in diamond calculated using the HSE06 and the PBE functionals. The HSE06 results for the NV$^-$ center is taken from Ref.[24].

System	Method	ZPL (eV)	A→B (eV)	C→D (eV)	ΔS (meV)	ΔAS (meV)
O_N-V_B	PBE	1.12	1.21	1.04	91	83
	HSE06	1.60	1.75	1.47	150	130
NV$^-$	PBE	1.74	1.93	1.58	189	160
	HSE06[24]	1.96	2.21	1.74	258	217
	Expt.[23]	1.95	2.18	1.76	235	185

The assignment of the GC-2 in c-BN center based only on the energy of the ZPL may not be convincing. More evidence comes from the phonon structure. Experimentally, a characteristic phonon energy of about 56 meV is observed in the cathodoluminescence spectra of the GC-2 defect center.[10, 12] Therefore, it would be very interesting to investigate the phonon structure of this defect center. Although rigorous quantum mechanical calculations of vibronic transitions of localized defect states is still not feasible today, the Franck-Condon principle provides a convenient theoretical foundation for identifying the local vibration modes (LVM) involved in electronic transitions. We identify the characteristic phonon energy involved in luminescence experiments in a few steps. First, we calculate the phonon structure of the O_N-V_B

center in a 216-atom supercell. All phonon modes, i.e., bulk phonons as well as the LVM, are calculated. Second, we identify the LVM associated with the defects using the localization measure $\xi_\alpha = \frac{\sum_i |\vec{p}_{\alpha i}|^4}{\sum_i |\vec{p}_{\alpha i}|^2}$, where $\vec{p}_{\alpha i}$ is the i^{th} atomic component of the polarization vector of the α^{th} phonon mode. This measure of the localization of phonon modes is similar to the inverse participation ratio (IPR) for measuring electronic localization. [25, 26] A phonon mode is identified as an LVM if its ξ_α is significantly greater than the averaged value. The LVM associated with the O_N-V_B center are listed in Table II. These results may serve as a guide for future experiments aimed at characterizing defects in c-BN.

TABLE II: Calculated LVM of the O_N-V_B center in c-BN and their Franck-Condon factors estimated by a projection procedure described in the text.

a_1 modes		e modes	
E (meV)	$\|\eta\|^2\times10^4$	E (meV)	$\|\eta\|^2\times10^4$
51.6	1.5	51.5	0.0
53.4	1.0	56.6	0.0
57.2	2.1	64.2	0.0
64.6	0.5	102.1	0.0
67.3	1.0	106.7	0.0
81.7	0.4	108.4	0.0
89.2	0.0	126.3	0.0
a_2 mode		128.2	0.0
132.6	0.0		

Next, we define a displacement vector between the structural configuration of the ground state and that of the excited states as

$$\Delta\vec{R}_i = [\vec{R}_i(Q_g) - \vec{R}_i(Q_e)]; i = 1, 2, \ldots, N, \quad (1)$$

where $\vec{R}_i(Q_g)$ and $\vec{R}_i(Q_e)$ are the positions of the i^{th} atom relaxed with the ground state and excited state occupations, respectively, as indicated in Fig. 4, and N is total number of atoms in the cell. Finally, we calculate the projection of the displacement vector onto the polarization vectors of the identified LVM:

$$\eta_\alpha = \sum_i \frac{1}{\sqrt{m_i}} \vec{p}_{\alpha i} \cdot \Delta\vec{R}_i, \quad (2)$$

where m_i is the mass of the i^{th} atom and $\vec{p}_{\alpha i}$ is the i^{th} atomic component of the polarization vector of the α^{th} phonon mode. Symmetry requires that the displacement vector $\{\Delta\vec{R}_i\}$ to have the a_1 symmetry. Therefore, only LVM with the a_1 symmetry will give a nonzero projection. The calculated projection $|\eta_\alpha|^2$ for the LVM are also listed in Table II. This projection should provide a faithful estimate for the Franck-Condon factor for the LVM involved in luminescence experiments. Figure 5 plots projections $|\eta_\alpha|^2$ versus the energy of the LVM. There should be at least six LVM involved in the luminescence spectra of the O_N-V_B center. The vibration pattern for a typical a_1 LVM is shown in the inset. To account for various broadening mechanisms, we apply a broadening of 3 meV for each LVM weighted by the projection $|\eta_\alpha|^2$, as shown with the dotted line in Fig. 5. The first three LVM together give rise to a prominent vibronic coupling peak at about 55 meV. This result compares very well with the experimental result of 56 meV for the GC-2 center.[10, 12].

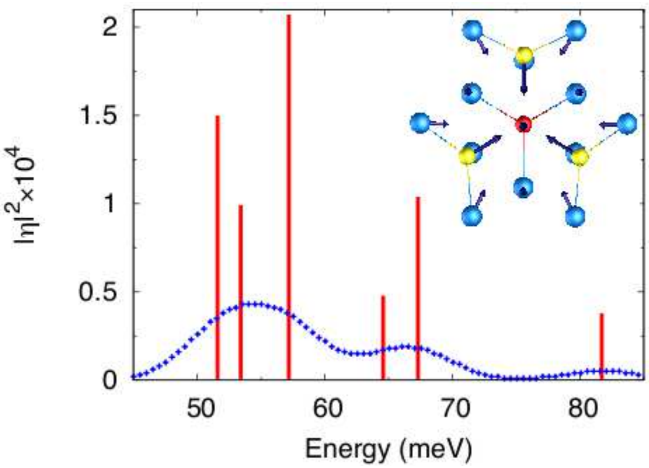

FIG. 5: Identified LVM phonon modes (vertical bars) and projection $|\eta_\alpha|^2$ weighted broadening (dotted line). These LVM are predicted to be strongly involved in the luminescence of the O_N-V_B center. The inset shows a vibration pattern for a typical a_1 LVM.

We would like to mention that the existence of singlet excited states [27–30] in the NV^-system plays a crucial role in the optical pumping mechanism. [31] Considering their similarities, one would expect that these singlet states also exist in O_N-V_B. However, further investigation is needed before we can draw a close comparison between the two color centers. The diamond NV^- also enjoys additional advantages such as the absence of nuclear spins for the ^{12}C isotope.

In conclusion, we have predicted a color center in c-BN which is isoelectronic to NV^- center in diamond. The defect complex consists of an oxygen substitution and an adjacent boron vacancy (O_N-V_B). Similar to the NV^- center, the defect states in the O_N-V_B center are well-localized and are optically accessible with a ZPL of about 1.6 eV. In addition, we find that this defect complex shares much of the characteristics of the often observed GC-2 center in c-BN. Vibronic coupling associated with the luminescence process of O_N-V_B is analyzed using a projection scheme within the Franck-Condon principle. The estimated vibronic coupling peaks at about 55 meV, which agrees well with observed characteristic phonon frequency (56 meV) of the GC-2 center in c-BN.

ACKNOWLEDGEMENT

The authors gratefully acknowledge Xuedong Hu for useful discussions. This work is supported by the US Department of Energy under Grant No. DE-SC0002623 (modeling of defects for electronics applications) and by the National Science Foundation under Grant No. DMR-0946404 (excited states of materials). Work at Beijing CSRC is supported by the National Natural Science Foundation of China (Grant No.11328401). We acknowledge the computational support provided by the Center for Computational Research (CCR) at the University at Buffalo, SUNY, and by the Center for Computational Innovations (CCI) at Rensselaer Polytechnic Institute.

[1] N. R. Jungwirth, Y. Y. Pai, H. S. Chang, E. R. MacQuarrie, and G. D. Fuchs, arxiv:1402.1773 (2014).

[2] P. B. Mirkarimi, K. F. McCarty, and D. L. Medlin, Materials Science and Engineering **R21**, 47 (1997).

[3] J. Ullmann, J. E. E. Baglin, and A. J. Kellock, J. Appl. Phys. **83**, 2980 (1998).

[4] H.-G. Boyen, P. Widmayer, D. Schwertberger, N. Deyneka, and P. Ziemann, Appl. Phys. Lett. **76**, 709 (2000).

[5] S. Matsumoto and W. Zhang, Jpn. J. Appl. Phys. **39**, L442 (2000).

[6] P. Ziemann, H.-G. Boyen, N. Deyneka, P. Widmayer, and F. Banhart, Pure Appl. Chem. **74**, 489 (2002).

[7] W. J. Zhang, I. Bello, Y. Lifshitz, K. M. Chan, Y. Wu, C. Y. Chan, X. M. Meng, and S. T. Lee, Appl. Phys. Lett. **85**, 1344 (2004).

[8] S. Eyhusen, C. Ronning, and H. Hofsäss, Phys. Rev. B **72**, 054126 (2005).

[9] V. D. Tkachev, V. B. Shipilo, and A. M. Zaitsev, Phys. Stat. Sol. (b) **127**, K65 (1985).

[10] V. D. Tkachev, V. B. Shipilo, and A. M. Zaitsev, Sov. Phys. Semicond. **19**, 491 (1985).

[11] A. M. Zaitsev, V. B. Shipilo, E. M. Shishonok, and A. A. Melnikov, Phys. Stat. Sol. (a) **95**, K29 (1986).

[12] V. B. Shipilo, A. M. Zaitsev, E. M. Shishonok, and A. A. Melnikov, J. Appl. Spectroscopy **45**, 1060 (1986).

[13] V. B. Shipilo, E. M. Shishonok, A. M. Zaitsev, A. A. Melnikov, and A. I. Olekhnovich, Phys. Stat. Sol. (a) **108**, 431 (1988).

[14] E. M. Shishonok, V. B. Shipilo, A. I. Lukomskii, and T. V. Rapinchuk, Phys. Stat. Sol. (a) **115**, K237 (1989).

[15] R. M. Erasmus and J. D. Comins, Phys. Stat. Sol. (c) **1**, 2269 (2004).

[16] S. Nistor, M. Stefan, D. Schoemaker, and G. Dinca, Solid State Commun. **115**, 39 (2000).

[17] S. V. Nistor, D. Ghica, M. Stefan, A. Bouwen, and E. Goovaerts, phys. stat. sol. (a) **201**, 2583 (2004).

[18] P. Giannozzi, S. Baroni, N. Bonini, M. Calandra, R. Car, C. Cavazzoni, D. Ceresoli, G. L. Chiarotti, M. Cococcioni, I. Dabo, et al., J. of Phys.: Conden. Matt. **21**, 395502 (2009).

[19] J. Heyd, G. E. Scuseria, and M. Ernzerhof, J. Chem. Phys. **118**, 8207 (2003).

[20] J. P. Perdew, K. Burke, and M. Ernzerhof, Phys. Rev. Lett. **77**, 3865 (1996).

[21] R. H. Wentorf, J. Chem. Phys. **36**, 1990 (1962).

[22] D. A. Evans, A. G. McGlynn, B. M. Towlson, M. Gunn, D. Jones, T. E. Jenkins, R. Winter, and N. R. J. Poolton, J. Phys.: Condens. Matter **20**, 075233 (2008).

[23] G. Davies and M. F. Hamer, Proc. R. Soc. London A **348**, 285 (1976).

[24] A. Gali, E. Janzén, P. Deák, G. Kresse, and E. Kaxiras, Phys. Rev. Lett. **103**, 186404 (2009).

[25] T. A. Abtew and D. A. Drabold, Phys. Rev. B **75**, 045201 (2007).

[26] R. Atta-Fynn, P. Biswas, and D. A. Drabold, Phys. Rev. B **69**, 245204 (2004).

[27] J. A. Larsson and P. Delaney, Phys. Rev. B **77**, 165201 (2008).

[28] A. Gali, M. Fyta, and E. Kaxiras, Phys. Rev. B **77**, 155206 (2008).

[29] Y. Ma, M. Rohlfing, and A. Gali, Phys. Rev. B **81**, 041204 (2010).

[30] S. Choi, M. Jain, and S. G. Louie, Phys. Rev. B **86**, 041202 (2012).

[31] V. M. Acosta, A. Jarmola, E. Bauch, and D. Budker, Phys. Rev. B **82**, 201202 (2010).